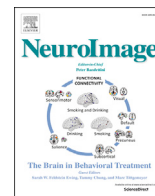




Contents lists available at ScienceDirect

NeuroImage

journal homepage: www.elsevier.com/locate/neuroimage

Strong health messages increase audience brain coupling

Martin A. Imhof^{a,c,*}, Ralf Schmäzle^b, Britta Renner^{a,c}, Harald T. Schupp^{a,c}

^a Department of Psychology, University of Konstanz, 78457, Konstanz, Germany

^b Department of Communication, Michigan State University, East Lansing, MI, 48824, USA

^c Centre for the Advanced Study of Collective Behaviour, University of Konstanz, 78457, Konstanz, Germany

ARTICLE INFO

Keywords:

Inter-subject correlation
ISC
EEG
fMRI
Health messages
Alcohol

ABSTRACT

Mass media messaging is central for health communication. The success of these efforts, however, depends on whether health messages resonate with their target audiences. Here, we used electroencephalography (EEG) to capture brain responses of young adults - an important target group for alcohol prevention - while they viewed real-life video messages of varying perceived message effectiveness about risky alcohol use. We found that strong messages, which were rated to be more effective, prompted enhanced inter-subject correlation (ISC). In further analyses, we linked ISC to subsequent drinking behavior change and used time-resolved EEG-ISC to model functional neuroimaging data (fMRI) of an independent audience. The EEG measure was not only related to sensory-perceptual brain regions, but also to regions previously related to successful messaging, i.e., cortical midline regions and the insula. The findings suggest EEG-ISC as a marker for audience engagement and effectiveness of naturalistic health messages, which could quantify the impact of mass communication within the brains of small target audiences.

1. Introduction

Mass media health campaigns are essential to promote public health. By using mass media, health agencies can reach millions and deliver messages about health risks and desired target behaviors (Rice and Atkin, 2013; Wakefield et al., 2010). A health issue for which this strategy is common is risky drinking, a significant problem among young adults and college students in particular (Karam et al., 2007; Slutske, 2005; Wicki et al., 2010). Typically, engaging audiovisual formats and mini-stories are used to make messages salient and increase personal risk perception, but many questions remain about how these messages affect recipients. Neuroimaging is particularly well suited to examine the reception process (Falk et al., 2015, 2016; Falk, 2010; Huskey et al., 2017; Wang et al., 2013; Weber et al., 2014). A promising approach to examine and quantify how audiences respond to dynamic real-life health messages, as for example videos, is the inter-subject correlation analysis (ISC). In brief, ISC measures the consistency of message-evoked brain responses across recipients, which yields a continuous, nonverbal measure of collective engagement that is well suited to quantify the impact of mass media messages at the neural level (Hasson et al., 2004, 2010, 2012).

Previous work using this approach, mostly within fMRI research,

demonstrated that manipulations of attentional and semantic variables influence the level of ISC across messaging contexts ranging from political rhetoric, to interpersonal communication, and to movie viewing (Hasson et al., 2008, 2012; Lahnakoski et al., 2014; Schmäzle et al., 2015; Silbert et al., 2014; Stephens et al., 2010). For example, using fMRI, Schmäzle et al. (2015) revealed enhanced ISC to political speeches which were perceived as powerful and engaging. Within the context of health and risk communication, two recent fMRI studies underscore the potential of the ISC approach for audience response measurement: The first study examined the reception of a 30-min documentary on the outbreak of the H1N1 swine flu virus that aired on national TV during the pandemic. The study revealed that the strength of fMRI-ISC in the anterior cingulate cortex depended on viewers' level of risk perception (Schmäzle et al., 2013). The second study showed that strength of ISC is related to the effectiveness of health messages (Imhof et al., 2017). Specifically, comparing fMRI-ISC during perception of strong and weak health messages, as defined by perceived message effectiveness in an independent sample, revealed enhanced ISC to strong messages in the dorsomedial prefrontal cortex, preceuneus, and the insulae. These studies illustrate the potential of an ISC-based neuroimaging approach to assess the reception of health messages with a focus on audience-wide responses that are critical for successful mass communication.

* Corresponding author. Department of Psychology, University of Konstanz, PO Box 36, 78457, Konstanz, Germany.

E-mail address: Martin.Imhof@uni-konstanz.de (M.A. Imhof).

<https://doi.org/10.1016/j.neuroimage.2020.116527>

Received 21 August 2019; Received in revised form 3 December 2019; Accepted 7 January 2020

Available online xxx

1053-8119/© 2020 The Authors. Published by Elsevier Inc. This is an open access article under the CC BY-NC-ND license (<http://creativecommons.org/licenses/by-nc-nd/4.0/>).

Here, we were interested in determining whether electroencephalography (EEG), for which a comparable ISC-based approach has been proposed (Cohen et al., 2017; Cohen and Parra, 2016; Dmochowski et al., 2012, 2014; Parra et al., 2018), can serve as a measure of audience engagement for health messages. One of the most important advantages of EEG is its temporal resolution, which ranges on the order of milliseconds. Thus, it complements hemodynamic measures, which offer good spatial but limited temporal resolution. Such a high temporal resolution is promising for characterizing the reception process of fast-paced audiovisual prevention messages, which often last only half a minute or less. Further benefits of EEG are its more accessible nature and relative cost-effectiveness. These characteristics enhance the scalability and thus the translational potential of integrating neuroscientific methods into message pre-testing, for example during the formative stages of a health campaign. Indeed, recent EEG studies in classroom settings, the cinema, or during music consumption illustrate this potential (Barnett and Cerf, 2017; Cohen et al., 2018; Dikker et al., 2017; Madsen et al., 2019; Poulsen et al., 2017).

The main goal of the present study was to determine whether EEG-ISC can robustly differentiate between strong and weak health messages and thus may serve as a possible marker of successful messaging. To obtain a sample of strong and weak messages, we screened German-speaking prevention campaigns on risky alcohol use. The video health messages obtained from this work were screened in terms of perceived message effectiveness, a widely used measure in health communication (PME; Dillard et al., 2007; Dillard and Peck, 2000). The messages revealed pronounced differences in perceived message effectiveness as well as other self-report measures of message characteristics (for details, please see section 2.2 or Imhof et al., 2017). Based on our previous work, we selected ten of the most and ten of the least effective video health messages to form strong and weak health message categories respectively. Dense sensor EEG was continuously recorded while participants viewed the messages. We then identified correlated components in the EEG signal to quantify the strength of ISC across the audience (Dmochowski et al., 2012; Parra et al., 2018) and to compare the strength of inter-brain coupling during reception of strong and weak messages. To determine the robustness of the findings, viewing conditions were varied between a free viewing task that resembled real-life viewing conditions and a rating task in which participants evaluated each message's effectiveness. Previous work suggested ISC as a proximal marker of audience engagement, due to attentional or relevance-based factors (Cohen et al., 2017; Dmochowski et al., 2012; Hasson et al., 2012; Imhof et al., 2017; Ki et al., 2016; Schmälzle et al., 2013). In addition, theories of media effects and persuasion assume that selective attention and elaborated processing of a message is crucial for changing attitudes or behavior – and can be brought out for instance by issue involvement, emotion, or personal relevance (e.g., Greenwald and Leavitt, 1984; McGuire, 2013; Petty et al., 2009; Petty and Cacioppo, 1986). Accordingly, we hypothesized that the degree to which recipients' brains respond similarly should be enhanced for strong as compared to weak health messages.

In a second line of analyses, we used both the acquired EEG-ISC and secondary fMRI data to identify the possible origin of the identified correlated components (see Dmochowski et al., 2014 - for a similar approach). In this analysis, fluctuations in ISC measured using EEG over the course of watching the health messages are used as predictors for functional imaging data which was collected in a second, independent sample viewing the same messages. One goal of this analysis was to identify which correlated EEG components show ISC primarily driven by visual-auditory stimulus characteristics. In addition, we assumed that distinct components can be related to the engagement of brain regions involved in personal relevance, affect and attentional processes, which are thought to be critical for effective health communication (e.g., Petty et al., 2009; Schmitz and Johnson, 2007). Accordingly, a further goal of this analysis was to test the hypothesis that a subset of correlated components has neural generators in higher-order cortical midline regions and the insula, which have been previously linked to affective- and

self-relevant processing of health-related messages (e.g., Imhof et al., 2017; Schmälzle et al., 2013). Moreover, message-evoked brain responses have been used to predict subsequent behavior change, such as smoking cessation or sunscreen use (Chua et al., 2009, 2011; Cooper et al., 2015; Falk et al., 2010, 2011). Thus, we additionally assessed changes in participants' drinking behavior over a four-week follow-up period. Using this data, we explored the hypothesis that EEG-ISC during health message exposure as well as self-report measures of risk perceptions and intentions to change behavior are related to changes in drinking behavior.

2. Material and methods

2.1. Participants

Thirty-two participants were recruited at the local university (16 female; between 18 and 34 years old, $M_{Age} = 22.69$, $SD = 4.32$). All participants had normal hearing, normal or corrected-to-normal vision, and no history of neurological or psychological diseases. One participant did not complete the four-week follow-up questionnaire. To be eligible for the study, participants had to report drinking amounts of at least four alcoholic beverages per week. Five additional participants were excluded due to technical failure or not fulfilling inclusion criteria (e.g., minimal drinking behavior or participation in earlier studies using a similar stimulus set). Excluded participants were not analyzed and immediately replaced to allow the full pre-determined sample size. We assessed the participants' drinking behavior using the AUDIT alcohol screening questionnaire (range: 0 – 40; Babor et al., 2001). All participants exhibited risky drinking patterns ($M_{Audit} = 11.31$; $SD = 4.61$; range: 5 – 24) according to a cut off recommendation for the German population (Rumpf et al., 2002). Participants received either course credit or monetary reimbursement. Written informed consent was obtained according to the Declaration of Helsinki and all procedures were approved by the ethics committee of the University of Konstanz.

2.2. Stimulus material

A sample of fifty German-speaking video health messages against risky alcohol use served as database from which 10 of the most and 10 of the least effective messages were selected to form a strong and a weak message category. Length of the messages varied between 20 and 110 s and did not differ between the two categories ($M_{Strong} = 58.5$ s, $SD = 25.93$; $M_{Weak} = 49.5$ s, $SD = 25.00$; $t(18) = 0.43$, *n.s.*, independent samples *t*-test, two-sided). These messages are the same as in our previous research using fMRI and a more detailed description can be found in Imhof et al. (2017). The video health messages obtained from this work were screened in terms of perceived message effectiveness (PME; Dillard et al., 2007; Dillard and Peck, 2000). The messages revealed pronounced differences in the previous work with respect to PME which was probed using single-item measures as well as questionnaires on ad effectiveness (Falk et al., 2012), perceived argument strength (Zhao et al., 2011), and perceived message sensation value (Palmgreen et al., 2002). As expected, assessing the current test audience's single-item evaluation of perceived message effectiveness confirmed the distinction into strong as compared to weak videos ($M_{Strong} = 4.88$, $SD = 0.98$; $M_{Weak} = 2.18$, $SD = 0.46$; $t(18) = 7.89$, $p < .0001$; $d = 3.53$, calculated using pooled *SD*; 95%-CI = 1.98 – 3.42; independent samples *t*-test, two-sided). Furthermore, the single-item PME ratings collected within the current EEG test audience were highly correlated to the ratings collected within the previous fMRI audience (Spearman's rank correlation coefficient $\rho = 0.96$, $p < .0001$).

2.3. Stimulus feature extraction and comparison across video categories

In order to assess whether the two categories of video health messages differed with regard to physical features, we assessed changes in video luminance, optical flow and sound envelope for each of the videos.

Analyses were conducted using the Computer Vision System Toolbox implemented in MATLAB. All videos were converted to greyscale by calculating the weighted sum of the R, G, and B components of each pixel. Then, stimulus features were extracted for each video frame: Luminance changes were extracted by calculating the squared difference in pixel intensity from one frame to the next and then averaged across pixels. Optical flow was computed using the Horn-Schunck method as implemented in the MATLAB Computer Vision System Toolbox. For each frame, the average across pixels of the magnitude of the optical flow vectors was calculated. As in [Dmochowski et al. \(2018\)](#), the sound envelope was computed as the squared magnitude of the Hilbert transform of the soundtrack accompanying the respective video health message. The extracted envelope was then downsampled to the video frame rate.

To match the resolution of the EEG-ISC, all stimulus feature time courses were smoothed using a 2 s Gaussian window and resampled to match the resolution of the ISC time course (2 s sliding window, 0.25 s increments) and z-scored. Finally, to assess whether frame-to-frame fluctuations of the physical stimulus features differ across video categories and to quantify the change over time for each stimulus feature, we compared the per-video averages (across samples) of the half-wave rectified time course of the first derivative, i.e., the absolute value of the derivative at a given sample point. In order to perform a sensitive comparison across video categories we compared the measures across categories using two-sided, uncorrected independent samples *t*-tests. There were no differences across video categories ($p = 0.68 - 0.37$, $t(18) = 0.42 - 0.93$). Box plots visualizing the average change of stimulus features as well as exemplary excerpts of the stimulus feature time courses for luminance changes, optical flow and sound envelope are shown in [Supplementary Figure SM 1](#).

2.4. Procedure

Prior to the experiment (t_1), we assessed EEG eligibility and collected alcohol-related self-report measures of drinking behavior and risk perceptions. In the main session (t_2), health messages were presented in a pseudo-randomized order, alternating between strong and weak exemplars. Videos were presented twice either in “forward” (A-B-C-...) or “reversed” order (...C-B-A). Presentation software (Neurobehavioral Systems, Inc.) was used to present the video health messages and to synchronize EEG acquisition. Videos were shown with a resolution of 800×450 pixels on a 27" flat screen monitor, located approximately 105 cm in front of the participant ($\sim 7.64^\circ$ visual angle vertically). Sound was delivered via speakers inside the shielded chamber. A 3 s video fixation was presented prior to each health message. In the “free viewing” block, participants were asked to attentively view the health messages, without any further task instruction. After each video, a blank screen (ITI = 5 s) was presented. In the “rating task” block, participants were asked to evaluate the health messages using a single-item measure of perceived message effectiveness on a seven-point scale. After logging the rating, a blank screen (ITI = 3 s) was presented. There was no difference for average rating time across health message categories ($M_{\text{Strong}} = 3.44$ s, $SD = 0.37$; $M_{\text{Weak}} = 3.65$ s, $SD = 0.34$; $t(18) = -1.38$, $p = 0.183$, *n.s.*, two-sided independent samples *t*-test). Order of task (free viewing vs. rating task) as well as the order in which the video health messages were presented (forward vs. reversed) was counterbalanced across participants. Overall, EEG measurements lasted for approximately 50 minutes with a short pause during the runs to allow for refreshment and re-measuring of electrode impedances. Self-reported risk perceptions related to alcohol were collected after the EEG session (t_2) and, using an online questionnaire, four weeks later (t_3). Additionally, in the follow up questionnaire, we again assessed drinking behavior and risk perceptions using the same items from the baseline measure at t_1 . With the exception of one, all participants completed the four week follow up questionnaire (average interval between t_2 and t_3 : 29 days, $SD = 3.4$). As in previous work, risk behavior and perceptions concerning alcohol use were assessed using self-report, i.e., detailed alcohol consumption, intentions, worries, perceived pressure to change behavior or perceived health threat ([Imhof](#)

[et al., 2017](#); [Renner, 2004](#); [Renner and Reuter, 2012](#); [Schmälzle et al., 2013](#)).

2.5. EEG acquisition and preprocessing

EEG and EOG scalp potential fields were measured with a 256-channel geodesic sensor net (EGI: Electrical Geodesics Inc., Eugene, OR, USA), sampled at 1000 Hz and on-line band-pass filtered from 0.01 to 400 Hz using EGI Geodesic amplifiers and Netstation acquisition software. Electrode impedance was kept below 40 k Ω , as recommended by EGI guidelines for this type of EEG amplifier. Data was recorded continuously with the vertex sensor (Cz) as reference electrode.

Data segments corresponding to the duration of each video health message were extracted using the open source signal processing toolbox FieldTrip ([Oostenveld et al., 2011](#)). Offline preprocessing of EEG and EOG data was conducted based on prior work (e.g., [Cohen and Parra, 2016](#); [Dmochowski et al., 2012](#); [Parra et al., 2018](#)). Specifically, EEG and EOG data were high-pass (0.5 Hz, Butterworth 6th order; forward/reverse) and notch filtered (50 Hz, Butterworth 4th order; forward/reverse). Eye movement artifacts were corrected by linearly regressing the EOG channels (EGI channels: 1, 10, 18, 25, 31, 32, 37, 46, 54, 226, 230, 234, 238, 241, 244, 248 & 252) from the EEG channels. Outlier samples were identified in each channel (magnitude exceeded four times the distance between the 25th and the 75th percentile of the signal). Samples 40 ms before and after outliers were replaced with zero values. Electrode channels with high variance (magnitude exceeded three times the distance between 25th and 75th percentile) were identified and replaced with zero values. These artifact rejection procedures were performed to discount outlier samples and channels in the subsequent calculation of covariance matrices and were used due to the sensitivity to outliers of the covariance matrices used in the ISC computation (see also [Cohen and Parra, 2016](#); [Dmochowski et al., 2012](#); [Parra et al., 2018](#)).

2.6. EEG-ISC analysis

EEG-ISC analysis was conducted based on the open source code developed by Parra and colleagues (available at <http://www.parralab.org/isc/>). Specifically, maximally correlated components were calculated, which represent linear combinations of scalp sensors revealing maximal correlation across viewers. In contrast to a voxel-by-voxel approach which is often used in fMRI-ISC analyses, the correlated components are calculated via signal decomposition. This spatial filtering enables to detect large-scale activity patterns which otherwise could remain unnoticed using a sensor-by-sensor approach ([Dmochowski et al., 2012](#)). To obtain unbiased estimates, correlated components were calculated using within- and between-subject covariance matrices that were averaged across all videos and viewings. Based on inspection of the eigenvalue distribution ([Supplementary Figure SM 2](#)) and previous work (e.g., [Cohen and Parra, 2016](#); [Dmochowski et al., 2012](#)), we extracted four components that captured most ISC. As in previous work, we visualize the spatial distribution of the components ([Fig. 2a](#)) by calculating the “forward models”, representing the covariance between a component’s activity and the activity at each sensor ([Cohen and Parra, 2016](#); [Dmochowski et al., 2012](#); [Haufe et al., 2014](#); [Parra et al., 2005](#)). To analyze experimental effects, EEG-ISC - as captured by the four components - was extracted for each video, the two task conditions and each participant, separately. Subsequently, ISC was averaged across strong and weak videos. Two-sided, paired samples *t*-tests were used to assess the main hypothesis of enhanced EEG-ISC for strong compared to weak health messages ([Fig. 2b](#)). Bonferroni correction was used to account for multiple comparisons. Confidence intervals as well as effect sizes are reported in [Supplementary Table SR 1](#). For paired samples *t*-tests, reported effect sizes represent Cohen’s d_z , calculated as the standardized mean difference effect size ([Lakens, 2013](#)).

In order to assess possible task and order effects we submitted the

EEG-ISC values for each component to four separate mixed repeated measures analysis of variance (ANOVA). Beside the within-subjects factor “Video Category” (strong/weak), we included the within-subjects factor “Condition” (rating task/free viewing) and the between-subjects factor “Order” (rating task followed by free viewing/free viewing followed by rating task) to test for possible influences due to the rating task and/or repeated viewings. Statistical analyses were conducted using jamovi software version 1.0.4.0 (<https://www.jamovi.org/>), R version 3.6.1 (<https://www.r-project.org/>), and the R packages “afex” (<https://cran.r-project.org/package=afex>) and “emmeans” (<https://cran.r-project.org/package=emmeans>).

2.7. Relating EEG-ISC to neural activation in independent functional neuroimaging data

In a second stream of analyses we calculated the EEG-ISC over time for each video and each of the components (2 s sliding window, 0.25 s increments). These ISC time courses were then used to predict neural activity measured in a second, independent target audience using fMRI. The fMRI data was taken from previous work in which an additional 32 participants (16 females, $M_{Age} = 23.41$; $SD = 2.96$) viewed the same alcohol prevention videos while neural data was acquired using a Siemens Skyra 3T MRI System (for details, see Imhof et al., 2017). Blood oxygenation level-dependent (BOLD) signal was acquired using a T_2^* -weighted Fast Field Echo-Echo Planar Imaging sequence (TR = 2.5 s, TE = 30 ms, ascending-interleaved slice order, 36 axial slices; no gap; FOV = 240 × 240 mm; 3 × 3 × 3.5 mm voxel size). 560 functional volumes were acquired during the audio-visual stimulation and scanning lasted approximately 45 min. Structural images were obtained using a T_1 -weighted scan (1 × 1 × 1 mm voxel size, FOV = 256 × 256 mm, 192 sagittal slices).

Neuroimaging data was preprocessed and analyzed using the BrainVoyager 20.4 software package (BrainInnovation). Functional data was corrected for slice scanning time (sinc-interpolation) and corrected for 3D Motion (trilinear/sinc-interpolation). The functional data was spatially smoothed (FWHM = 6 mm) and temporally filtered to remove linear trends and low-frequency shifts using a high pass-GLM-Fourier filter (up to 6 cycles). Functional and anatomical volumes were normalized into the Talairach coordinate system (Talairach and

Tournoux, 1988). As visualized in Fig. 1, EEG-ISC time courses were extracted separately for each component and the first viewing of each video. For each of the four components, EEG-ISC time courses corresponding to the first viewing of each of the 20 videos were extracted separately. Then, these 80 time courses were each resampled to a 1 s resolution and z-scored. For each component, the time courses of the 20 single videos were concatenated to serve as one parametric predictor in four separate general linear model (GLM) analyses. Periods of fixation and inter-stimulus intervals were modeled as zero estimates and included in the parametric regressors. Within each of the four multi-subject random effects GLM analyses we included the respective parametric regressor convolved with a default two gamma-HRF as implemented in BrainVoyager (time to response peak: 6 s, no shift) and default treatment for temporal autocorrelation (second-order autoregressive). Lastly, contrasts of parameter estimates were constructed as null hypothesis tests of the parametric regressor against zero (two-sided). To correct for multiple comparisons, we applied FWE correction ($p < 0.05$, whole brain) and a cluster threshold of 25 mm². All results shown in Figs. 3 and 4 are overlaid onto the left hemisphere of a Talairach-normalized, anatomical rendering of the Colin27 Average Brain (Holmes et al., 1998). Right hemisphere results are very similar and are visualized in Supplementary Figure SR 2.

To quantify the overlap between the current fMRI-GLM results and previous fMRI-ISC findings, we created statistical maps that include the voxels which revealed a significant relationship to the parametric regressor of the respective correlated EEG component (as shown in Fig. 3/ Fig. 4a). Then, we combined the statistical maps previously published in Imhof et al. (2017), which include all voxels that revealed significant fMRI-ISC during either the strong or the weak messages (Fig. 4b). Finally, we used these maps to determine the degree to which the voxels found in the EEG-ISC informed fMRI analysis revealed overlap with the combined fMRI-ISC map (Fig. 4c).

2.8. Assessing changes in drinking behavior and their relations to EEG-ISC

We determined changes in alcohol consumption and risk perception following the exposure to the health messages using two-sided, paired samples *t*-tests. Furthermore, multiple linear regression analysis was used to explore the ability of EEG-ISC to predict changes in subsequent

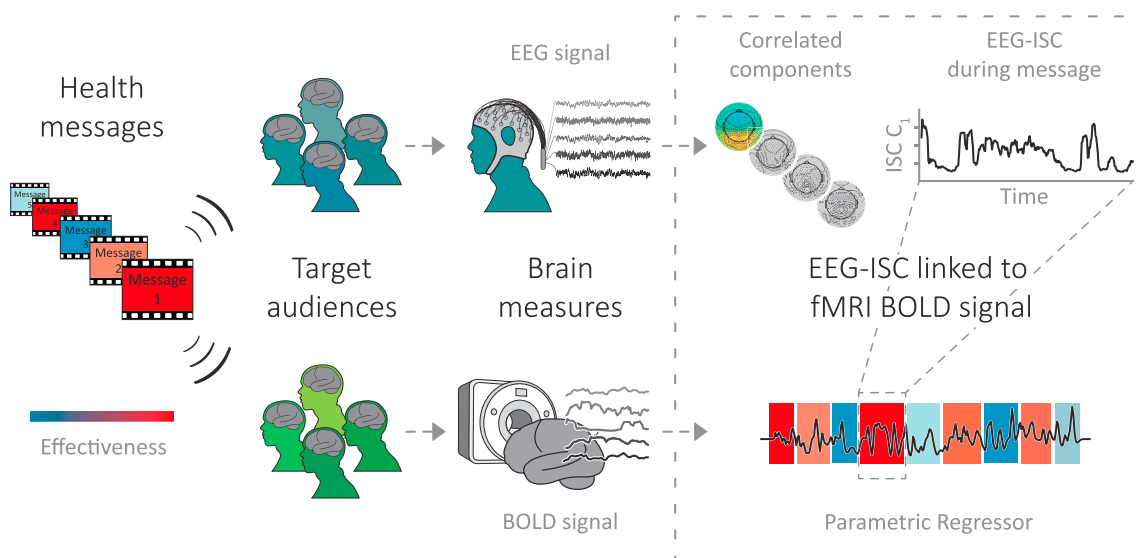


Fig. 1. Conceptual overview of the EEG-ISC informed fMRI analysis. Brain responses of two independent audiences are obtained during watching real-life video health messages. Temporally highly-resolved EEG-ISC time courses are extracted for maximally correlated EEG components. The ISC time courses obtained from the EEG sample are then used as parametric regressors in a general linear model design modeling the BOLD signal within the whole brain. The BOLD signal modeled in this design was obtained during message reception of the same video health messages within a second, independent sample of participants.

drinking behavior. In two linear regression models, amount and frequency of drinking at follow up were dependent variables. The corresponding drinking measure at baseline, self-reported risk perceptions (worries, need to act, intentions and perceived health threat), as well as level of EEG-ISC averaged across the 10 strong health messages for each of the components, were entered as independent variables (for the full

model description, see Supplementary Table SR 6). We used R version 3.6.1 to create the multiple linear regression models and subsequently computed hierarchical linear regression to infer the amount of additionally explained variance for the predictors-of-interest as reported in Table 1.

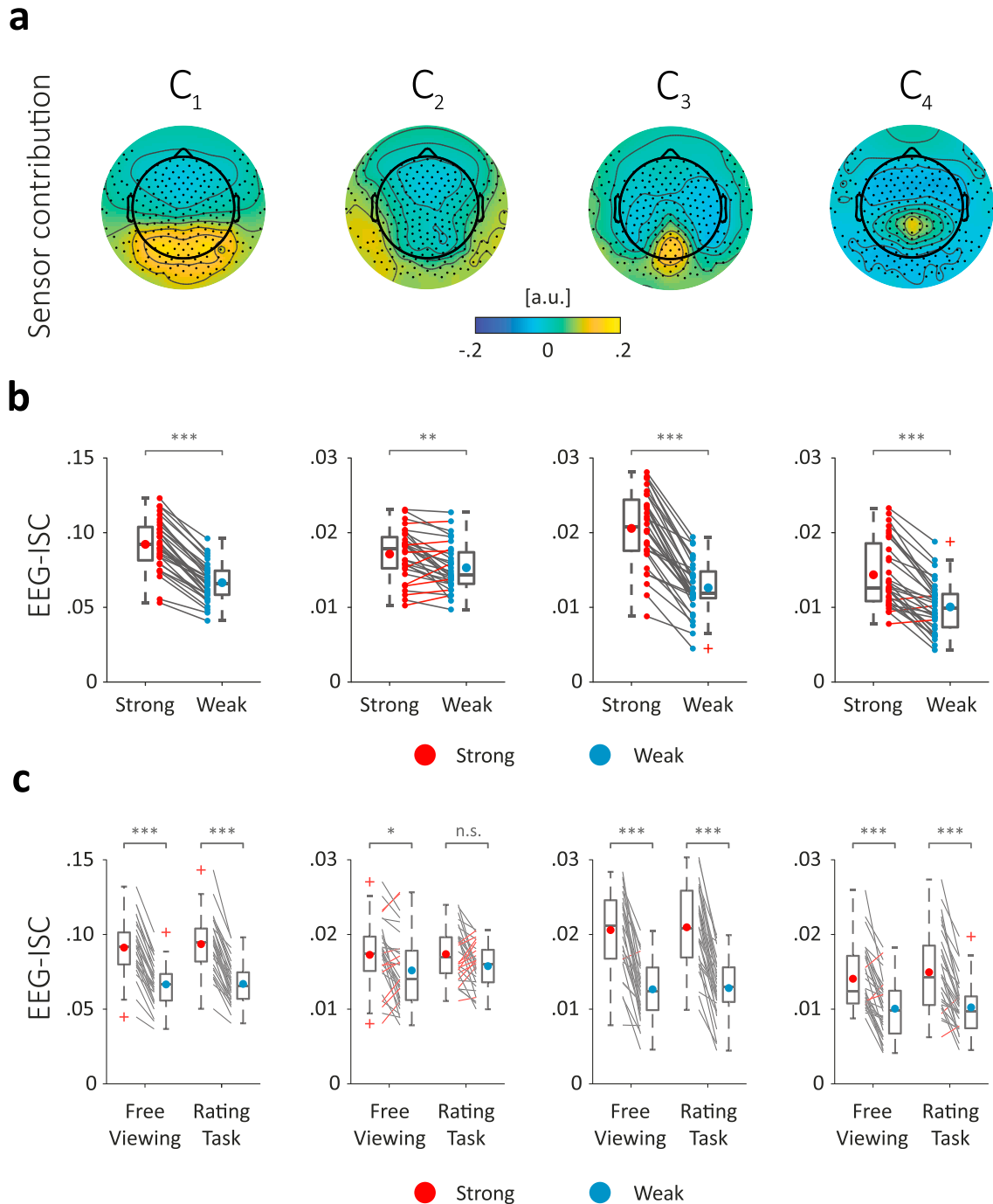


Fig. 2. Maximally correlated EEG components reveal differences in ISC during the viewing of alcohol prevention videos. a) Topographical maps visualize the strength to which each sensor contributes to the correlated component. The maps reveal the contribution by showing interpolated magnitudes of the scalp projections, that is, the forward models of the maximally correlated components C_1 to C_4 (blue to yellow - arbitrary units, polarity of projections normalized). b) Box plots show average EEG-ISC for each component, separated by the message categories Strong (red) and Weak (blue). Connecting lines visualize paired measures for all 32 participants. Participants exhibiting a reversed pattern of results ($ISC_{Weak} > ISC_{Strong}$) are colored red. c) Stability of EEG-ISC differences is revealed by replicable differences when assessing the data on a more fine-grained level, i.e., during free viewing and a rating task. Box plots show ISC for each component as a function of message category and viewing condition. Colored dots within box represent the mean, center lines the median, edges represent the 25th & 75th percentiles and outliers are marked by a red cross. For descriptive purposes, significance of paired samples *t*-tests comparing the two video categories are shown for each experimental cell (* $p < .05$, ** $p < .01$, *** $p < .001$; Bonferroni corrected).

3. Results

3.1. Strong health messages prompt enhanced audience brain coupling

To examine the degree of inter-brain coupling within the audience prompted by strong compared to weak health messages, we exposed a test audience of 32 viewers to video health messages while measuring high-density EEG. In the current work, the video health messages were evaluated regarding perceived message effectiveness (PME; Dillard et al., 2007; Dillard and Peck, 2000) and other message-relevant constructs in previous work (Imhof et al., 2017; see section 2.2 for details). Differences in effectiveness were confirmed in the present sample. ($M_{\text{Strong}} = 4.88$, $SD = 0.98$; $M_{\text{Weak}} = 2.18$, $SD = 0.46$; $t(18) = 7.89$, $p < .0001$; $d = 3.53$, independent samples t -test, two-sided).

In order to calculate inter-subject correlation (ISC) across viewers, we extracted the four most correlated components of the EEG data. Fig. 2a visualizes which sensors contribute to the correlated components and reveals distinct topographies for each component using their forward projections. To confirm the hypothesis that strong compared to weak health messages prompt enhanced inter-brain coupling across the audience, we submitted the level of ISC to paired samples t -tests, which confirmed the hypothesis for all identified components (C_1 : $t(31) = 18.18$, $d = 3.21$; C_2 : $t(31) = 4.14$, $d = 0.73$; C_3 : $t(31) = 13.94$, $d = 2.46$; C_4 : $t(31) = 9.15$, $d = 1.62$; all p 's < 0.001 , two-sided, Bonferroni corrected; for details, please see Supplementary Table SR 1). As illustrated in Fig. 2b, the enhancement of ISC for strong health messages was highly consistent across viewers, i.e., the pattern was expressed in every audience member for C_1 and C_3 (32 out of 32), and in 29 out of 32 participants for C_4 . Although still significant, the effect appeared less consistent for C_2 with 24 out of 32 participants. Moreover, when computing the correlated components separately for each of the video categories and viewings, the spatial topographies of the components were stable across viewings but revealed seemingly more heterogeneity for weak messages (see Supplementary Figure SR 1). In sum, strong health messages led to a robust enhancement of inter-brain coupling as measured by EEG-ISC.

3.2. Enhanced inter-brain coupling to strong messages during free viewing and an effectiveness rating task

In a second step, we examined whether the pattern of enhanced ISC for strong messages varied across viewing conditions, that is, free viewing and an active rating task in which participants evaluated message effectiveness. For each component, possible task and order effects were assessed via four separate mixed repeated measures analyses of variance (ANOVAs) with the within factors "Video Category" (strong vs. weak) and "Condition" (free viewing vs. rating task), and the between factor "Order" based on the sequence of the two conditions, which was counterbalanced across viewers.

As shown in Fig. 2c, inter-brain coupling, as measured by the level of ISC for the four components, was enhanced for strong compared to weak messages during both task conditions (Main effects of "Video Category": $F(1,30) = 16.61 - 321.04$; all p 's < 0.001 , $\eta^2_G = 0.06 - 0.43$; for details, see Supplementary Table SR 2). The main effects of video category were not qualified by any higher-order interaction in the separate ANOVAs of C_1 , C_2 , and C_3 . For C_4 , the interaction of "Video Category x Condition x Order" reached significance ($F(1,30) = 7.10$, $p = .012$, $\eta^2_G = 0.01$). However, two separate follow up-mixed repeated measures ANOVAs of both the free viewing and the rating task condition data revealed only significant main effects of video category (Free viewing: $F(1,30) = 51.04$, $p < .0001$, $\eta^2_G = 0.21$; Rating task: $F(1,30) = 62.89$, $p < .0001$, $\eta^2_G = 0.22$). No other significant effect was found in these separate analyses. For C_1 and C_2 , level of ISC decreased from first to second viewing across both task orders resulting in significant interactions of "Condition x Order" (C_1 : $F(1,30) = 46.55$, $p < .0001$, $\eta^2_G = 0.08$; C_2 : $F(1,30) = 11.80$, $p = .002$, $\eta^2_G = 0.07$). Overall, the degree of EEG-ISC prompted by strong messages was consistently enhanced compared to weak messages - during both free

viewing and the evaluation task. This pattern was especially pronounced for components C_1 , C_3 and C_4 . Moreover, to allow a comparison to previous research (Cohen and Parra, 2016; Dmochowski et al., 2014), an additional analysis using the same statistical model but ISC summed across the four components was computed which revealed similar results (Supplementary Table SR 3).

3.3. Relation between EEG-ISC and fMRI signal

To identify candidate brain sources of the maximally correlated components, we used the temporally resolved EEG-ISC responses to model fMRI data obtained during viewing the same health messages. Critically, EEG and fMRI data were recorded from two independent audiences exposed to the same messages, so that data can be integrated across groups (see Dmochowski et al., 2014; Haufe et al., 2018 - for similar approaches). Specifically, the EEG-ISC time courses from each of the four previously identified components were used as a parametric regressor in separate GLM-analyses modeling the fMRI data (see Fig. 1). In other words, we asked where in the brain the temporal variation of EEG-ISC across the first audience tracked with blood-oxygen-level-dependent (BOLD) signal in the second audience.

As shown in Fig. 3, the results of the four identified EEG components reveal overlap, but they also show distinct patterns for each of the components. The results show that all four components tracked with BOLD signal in primary visual and auditory cortices as well as unimodal and heteromodal associative cortices (e.g., Mesulam, 1998). Importantly, significant relations between EEG-ISC and BOLD signal extended beyond sensory-perceptual regions. Specifically, BOLD signal within the posterior cingulate cortex (PCC) tracked with EEG-ISC of components C_2 and C_4 . Furthermore, signal in the insula and the precuneus was related to EEG-ISC of components C_3 and C_4 . Finally, EEG-ISC of component C_4 was additionally related to the fluctuation of BOLD signal within the anterior cingulate (ACC), and dorsomedial prefrontal cortex (dmPFC). Previous research related these higher-order brain regions to personal relevance, affect and attentional processes (Etkin et al., 2011; Murray et al., 2012; Qin and Northoff, 2011; Raichle, 2015; Schmitz and Johnson, 2007; Shackman et al., 2011).

3.4. Correspondence between EEG-ISC and fMRI-ISC findings

In addition to providing information on the potential neural generators of EEG-ISC, the EEG-informed fMRI analysis allows to assess the correspondence of our ISC results across two neuroimaging modalities. To facilitate comparison, Fig. 4 enables to compare the current findings to previous fMRI-ISC findings during processing the same strong and weak health messages (Imhof et al., 2017). Similar to our previous work, the neural regions that show a relation to the identified correlated EEG components extended itself across the cortical hierarchy from "basic" sensory-related to "higher-order" cortical regions (e.g., Mesulam, 1998). When comparing the statistical maps of the two separate streams of analyses, we find that more than 90% of the current findings of the EEG-informed fMRI analysis revealed overlap with the fMRI-ISC findings of the previous work. Given the cross-experimental nature of data acquisition and analysis, marked parallels are found when comparing fMRI-ISC analysis and possible neural generators of the correlated components in the current data.

3.5. Relationship between EEG-ISC and change in drinking amount

In a first step, we determined whether there was any change in alcohol consumption following exposure to the health messages. At the group level, an overall reduction compared to the baseline before exposure to the health message was seen in amount and frequency of drinking within the follow up questionnaire (Amount $t(30) = 3.11$, $p = .004$, $d = 0.56$; Frequency: $t(30) = 3.00$, $p = .005$, $d = 0.54$; $N = 31$, paired samples t -tests, two-sided, uncorrected - for details, see Supplementary Information,

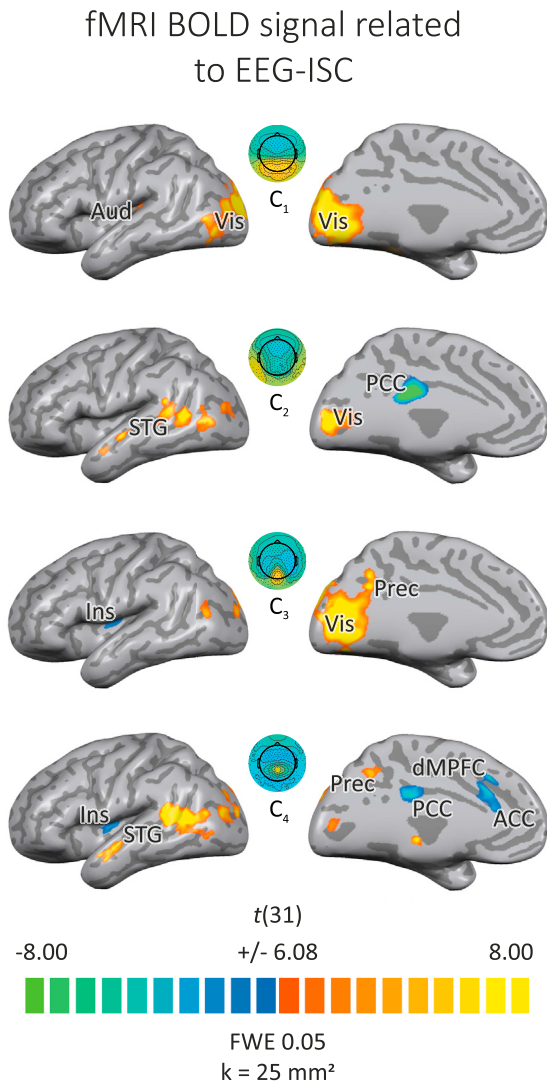


Fig. 3. Results of EEG-ISC informed fMRI analyses reveal distinct regions in which BOLD signal tracked with the ISC of correlated EEG components. a) EEG-ISC fluctuations co-vary with BOLD signal in sensory-perceptual and higher-order brain regions. Illustrations show results of GLM analyses in which ISC time courses of the correlated components obtained in EEG analysis were used as parametric regressors predicting BOLD signal (t -values, FWE corrected for multiple comparisons, $p < .05$; 25 mm² voxel contiguity). ACC = Anterior cingulate cortex, Aud = Auditory cortex, dmPFC = Dorsomedial prefrontal cortex, Ins = Insula, PCC = Posterior cingulate cortex, Prec = Precuneus, STG = Superior temporal gyrus, Vis = Visual system. All visualizations are shown on Talairach-normalized anatomical renderings of the left hemisphere.

Table SR 5). With regard to the amount of drinking, participants on average reported to drink 3 or 4 beverages per drinking event at follow up,

Table 1

Results of Hierarchical Regression: Predicting Amount of Drinking at Follow Up using Self-Report Measures Alone and then Combining Self-Report Measures with Inter-Brain Coupling.

Step	R^2	Adj. R^2	Res. DF	F values	Model sig.	R^2 change	F change	F change sig.	AIC
1: Drinking amount at Baseline	.42	.40	29	20.86	$8.435 \cdot 10^{-5}$				56.42
2: Self-report	.67	.60	25	9.95	$2.498 \cdot 10^{-5}$.247	5.74	.003 **	47.27
3: Brain coupling C ₃ and C ₄	.76	.69	23	10.63	$6.418 \cdot 10^{-6}$.098	4.57	.022 *	40.47
4: Brain coupling C ₁ and C ₂	.77	.68	21	7.99	$4.668 \cdot 10^{-5}$.010	0.46	.636	43.13

Notes. R^2 = Multiple R squared, Adj. R^2 = Adjusted R squared, Sig. = Significance. Significance codes: *** $p < .001$, ** $p < .01$, * $p < .05$. Self-report measures: Worries, need to act, intentions & perceived health threat.

corresponding to a lowering of half a scale point. There were no changes in binge drinking or self-report measures probing alcohol consumption on a weekly resolution, that is, the week prior to baseline compared to the week prior the follow up questionnaire. Specifically, participants consumed on average 8.32 standard beverages ($SD = 5.25$) in the week prior the baseline and 7.90 beverages ($SD = 8.38$) in the week prior to the follow up questionnaire ($t(30) = 0.24, p = .810, n.s.$ - see Table SR 5 for details).

In a second step, we used linear regression to explore whether neural measures of health message processing as well as self-reported risk perceptions were related to changes in drinking behavior. Significant effects were seen with regard to amount of drinking, but not for drinking frequency. In a linear regression model, ISC averaged across strong health messages for components C₁ to C₄, drinking at baseline, as well as self-reported drinking-related worries, intentions, perceived need to act, and perceived health threat were entered as independent variables, resulting in a significant model for amount of drinking ($F(9,21) = 7.99, p < .0001$; adj. $R^2 = 0.68$). In this model, ISC as captured by components C₃ and C₄, baseline drinking, and self-reported need to act, intentions, and perceived health threat, were significant predictors of drinking at follow up (p 's = 0.03 to < 0.001 ; for details, see Supplementary Table SR 6).

Lastly, to determine whether neural measures can make a unique contribution, we computed a hierarchical linear regression analysis. First, we entered amount of drinking at baseline followed by worries, need to act, intentions to change, and perceived health threat which explained an additional 24.7% of variance ($F_{change} = 5.74, p = .003$). Entering ISC of components C₃ and C₄ in the next step explained an additional 9.8% of variance resulting in a better model fit ($F_{change} = 8.71, p = .002$ - see Table 1). Adding EEG-ISC of components C₁ and C₂ did not explain additional variance.

4. Discussion

Health messages are critical for health promotion and disease prevention, but only if they reach and positively engage their target audience. To achieve this at scale, however, messages must be able to attract and sustain attention of the recipients – and collectively across large audiences. Here, we presented members of a target audience with real-life video health messages about risky alcohol use and assessed the collective coupling across their brains during message exposure using inter-subject correlation (ISC). We find that the strength of audience-wide ISC during message receipt is associated with the strength of the messages, that is, their perceived effectiveness. Our findings imply that the strength of ISC within an audience can indicate whether a health message resonates across receivers. Capturing these effects across the brains of an audience may thus provide a promising tool to objectively quantify the impact of mediated health messages and for studying the micro-level processes in response to persuasive messages.

4.1. Strong health messages increase audience brain coupling

The main finding is that strong health messages increased inter-brain coupling across the audience. When our test audience was exposed to strong messages, the receivers' brain responses became more closely aligned, whereas messages that people evaluated as being less effective

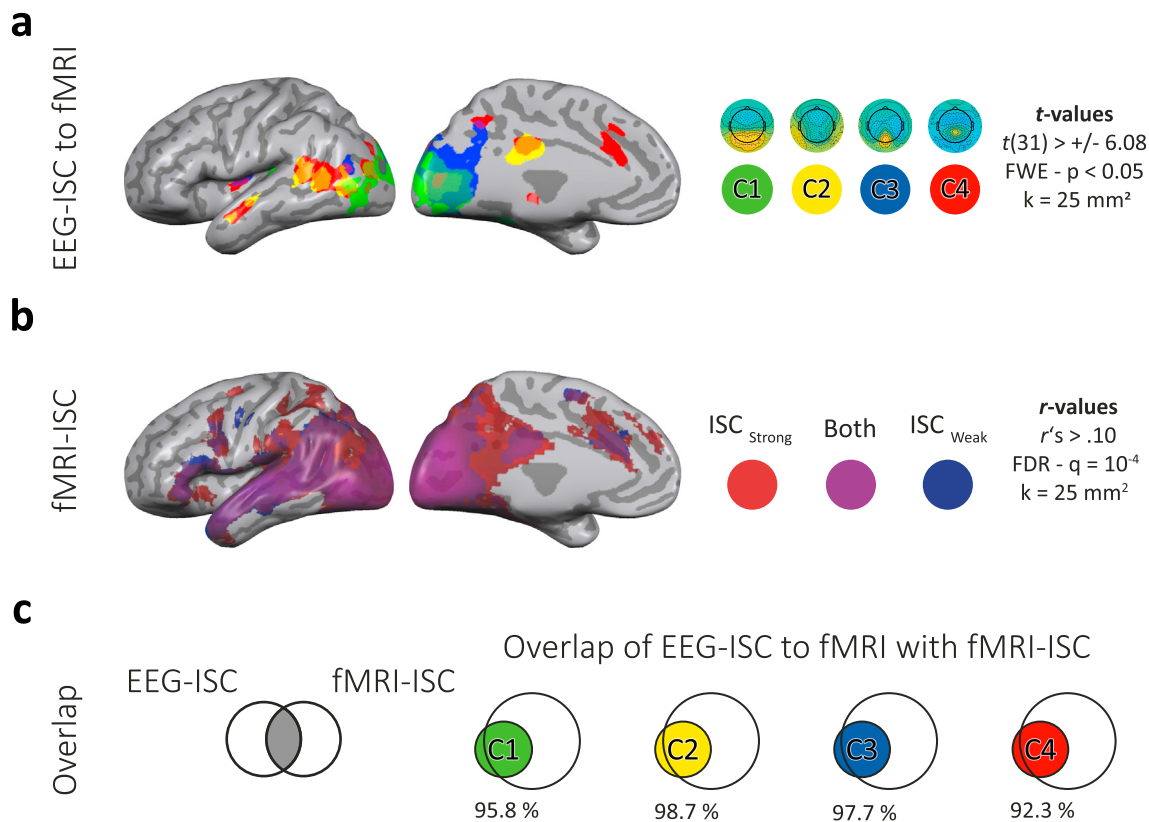


Fig. 4. Correspondence between EEG-ISC related to fMRI signal and fMRI-ISC findings from previous work. a) Results of EEG-ISC informed fMRI analyses reveal regions in which BOLD signal tracked with EEG-ISC. Illustrations show results of GLM analyses in which ISC time courses of the correlated components obtained in EEG analysis were used as parametric regressors predicting BOLD signal (t -values, FWE corrected). b) fMRI-ISC results from Imhof et al. (2017) obtained in an independent participant sample that viewed the same video health messages. R -values obtained in fMRI-ISC analysis are overlaid onto the same anatomical rendering for Strong (red) and Weak (blue) messages (FDR corrected). All visualizations are shown on a Talairach-normalized anatomical rendering of the left hemisphere. c) A large portion of the voxels shown in the statistical maps depicted in a) reveals overlap with the voxels depicted in the statistical maps in b) - for details, please see section 2.7).

evoked more heterogeneous responses. This effect was found for all identified components and corroborated across two experimental tasks. Our findings are in line with a growing body of research that uses fMRI and EEG to assess the neural base of audience engagement in response to naturalistic stimuli, such as rhetorically strong speeches, engaging movies, or narratives (Barnett and Cerf, 2017; Cohen et al., 2017; Cohen and Parra, 2016; Hasson et al., 2010; Honey et al., 2012; Ki et al., 2016; Lahnakoski et al., 2014; Schmälzle et al., 2015; Silbert et al., 2014). Importantly, the components C₁, C₃ and C₄ found in the present work closely resembled components obtained in previous studies using naturalistic audio-visual stimuli, but different tasks, EEG-systems, and sensor layouts (e.g., Cohen and Parra, 2016; Dmochowski et al., 2012). Recent evidence suggests that correlated EEG components - similar to ISC in fMRI (Schmälzle et al., 2015) - can track attentional and behavioral engagement in an audience (Cohen et al., 2017; Dmochowski et al., 2012, 2014; Ki et al., 2016). This extension of the ISC approach to EEG is promising since it allows a more flexible measurement in real world contexts and thus offers translational potential for neural measures as a scalable assessment of the audience response to health media.

4.2. Using EEG-ISC to study real-life health media

While studying naturalistic stimuli increases ecological validity it also raises the issue that real-life health messages may not only differ with regard to content characteristics but also with regard to physical properties. To gain insights into this issue, we extracted changes in luminance, optical flow and sound envelope for each of the videos and found that strong and weak health messages did not significantly differ with regard

to these features in the current study (see section 2.3). However, given the multitude of possible physical features, only a systematic experimental variation of physical and psychological features of messages can solve this issue conclusively.

With respect to content-based characteristics, real-life messages often differ along a number of variables such as message sensation value or argument strength - which is also the case in the current sample of messages (see section 2.2). More fine-grained analyses of health messages are needed to tackle the challenge of relating ISC-based neural engagement metrics to dynamic message contents and tactics. Given the excellent time resolution, EEG-ISC appears well-suited to identify crucial elements of a message that drive collective audience responses. For example, the proposed measure may answer on a scene-by-scene level to what extent neural engagement is driven by fear appeals and dramatic imagery, and also how these content characteristics interact with physical properties, such as stimulus dynamics or intensity. Moreover, recent work linked think-aloud protocols captured immediately after message exposure to brain activity (Pei et al., 2019) and a similar strategy would be feasible for ISC-based approaches (cf. Dmochowski et al., 2012). We anticipate that ISC could indicate if moments of a video or specific elements of the messages “got under the skin” of the recipients and predict upcoming verbal elaborations by recipients that became affectively engaged. Future research may now delve into the contents of messages and examine how variations in the presented arguments or employed message tactics affect the ISC-based engagement metrics. Overall, it may be feasible to include EEG measures in the formative stage of health campaigns to identify, design and pre-test elements of health messages, as is already the case for eye-tracking to optimize spatial attention

allocation (Lochbuehler et al., 2016).

4.3. EEG-ISC informed fMRI analyses reveal brain regions related to correlated EEG components

In addition to providing a neural measure of audience engagement, the integration of EEG-ISC and fMRI suggests that the correlated components found in EEG data may tap into distinct functional brain systems. The EEG-informed fMRI analyses identified several brain regions involved in sensory and perceptual analysis, but also revealed the anterior and posterior cingulate cortex (ACC & PCC), the dorsomedial prefrontal cortex (dmPFC) and the insula - regions, which are involved in a broad array of functions relevant to successful messaging and persuasion. These results align with the work of Dmochowski et al. (2014) who similarly observed relations between EEG-ISC and BOLD signal for the reception of commercials using an fMRI block-design within superior temporal, inferior frontal and cortical midline regions. Importantly, a robust differentiation of strong and weak health messages emerged in the current study for ISC of components C₃ and C₄, components which the EEG-fMRI correspondence analysis related to cortical midline regions (C₄) as well as to the insula and the precuneus (C₃ & C₄). Numerous fMRI studies have linked these cortical midline regions to a broad set of processes including assessments of personal relevance as well as social and memory-related tasks, and affective evaluation (Apps et al., 2016; D'Argembeau et al., 2010; Etkin et al., 2011; Murray et al., 2012; Qin and Northoff, 2011; Raichle, 2015; Schmitz and Johnson, 2007; Shackman et al., 2011). Furthermore, the insula and ACC have emerged as key nodes in the so-called salience network, which is, together with the PCC, supposedly involved in tuning attention to internal or external information and shifting working-memory resources (Leech and Sharp, 2014; Menon and Uddin, 2010; Raichle, 2015; Seeley et al., 2007). While acknowledging the limits of reverse inference (Poldrack, 2006), the picture that arises based on the current findings and previous work (Imhof et al., 2017; Schmäzle et al., 2013, 2015) is that during strong messages, ISC across an audience is consistently enhanced across multiple recipients, not only within stimulus-driven brain regions, but also within regions related to higher-order processing - such as assessing personal relevance, affective evaluation and attention.

4.4. Inter-subject correlation as a possible marker of message success

From a communication perspective, the correlated brain responses exposed by our analyses represent the common effects of messaging, that is, the degree to which a given message aligns neural processing across multiple receivers. To state the obvious: without a message acting as an "audience-aligner", brain activity across persons is basically uncorrelated (Hasson et al., 2004, 2008). Furthermore, when messages are unengaging or compromised in their meaning, e.g., by presenting unintelligible reversed speech to audiences, then correlated brain activity is relatively weak and confined mostly to sensory areas (Honey et al., 2012; Schmäzle et al., 2015). Thus, we can think of the degree of message-evoked ISC along a continuum ranging from unaligned to strongly aligned (Hasson et al., 2004, 2008, 2010). On that view, strong health messages were more effective in the sense that they prompted a stronger shared signal in the audience. The EEG-informed fMRI analyses implied that this effect is linked to self-relevance and attentional processes. This finding is particularly promising because personal relevance and the ensuing involvement or central processing represent key constructs in the persuasion literature (e.g., Greenwald and Leavitt, 1984; Petty et al., 2009; Petty and Cacioppo, 1986). Along similar lines, multiple theories in health psychology and risk communication suggest that conveying an authentic feeling of "being personally at risk" is central to successful health messaging (Ferrer and Klein, 2015; Renner et al., 2015; Slovic and Peters, 2006; Weinstein, 1989). Taken together, audience brain coupling of EEG and fMRI can reveal if and how health messages align and prompt shared signal across members of a target audience. By

exploiting this ability, the strength of ISC may serve as a proximal marker of health message success.

Identifying such markers of health message success can inform health communication research focused on designing more effective messages. For example, the present findings relate to a recent debate on the usefulness of perceived message effectiveness (PME) for selecting messages that are likely going to be successful. In brief, PME-scales have been used in formative research based on the assumption that they can serve as a proxy for actual effectiveness (Dillard et al., 2007; Yzer et al., 2015). However, recent work by O'Keefe (2019, 2018) argued that PME is not demonstrably related to actual effectiveness in meta-analyses (but see Cappella, 2018; Davis and Duke, 2018). Our results speak to this debate insofar as they show that messages evaluated as high in perceived effectiveness by the participants of our screening sample actually prompted stronger ISC of EEG data in another, independent test audience. Furthermore, exploratory analysis showed that EEG-ISC was predictive of behavior change. Acknowledging that these findings await replication by future research, it can be argued that messages that prompt a stronger initial audience response are more likely to be successful (McGuire, 2013) - whether in the participants who are being tested or in new audiences, including the population level targeted by mass-media campaigns (Dmochowski et al., 2014; Falk et al., 2015, 2016; Huskey et al., 2017; Weber et al., 2014). Considering that mass media health messages can reach large populations, even relatively small advantages in audience engagement may lead to consequential differences in audience impact.

Demonstrating that inter-subject correlation can be reliably measured with EEG is relevant for the issue of group and cultural differences in designing health messages. Empirical evidence demonstrated that message variables can interact with personal variables, such as issue involvement, prior experience, or attitudes towards certain topics, and this can cause differences in neural processing of health messages (Weber et al., 2013, 2014). Given that EEG is comparatively cheap and can be measured with mobile devices, EEG-ISC may provide means to better assess the targeting of messages to different groups (e.g., Chua et al., 2011; Chua et al., 2009), to make samples less "WEIRD" (Burns et al., 2019; Henrich et al., 2010) and thus, on the long term more generalizable.

4.5. Inter-subject correlation as a possible predictor of message effects

The ultimate goal of health communication is to influence health by successfully informing and persuading people to reduce risky behaviors or engage in preventive action. To help with this endeavor, the EEG-ISC approach may offer a marker of messaging success (Dmochowski et al., 2014). In the current study, EEG-ISC of components C₃ and C₄ was not only related to higher-order brain regions but did also, in addition to self-report measures, predict reductions in risky drinking. By contrast, adding EEG-ISC of components C₁ and C₂, whose neural generators were most likely located in brain regions devoted to sensory and perceptual analysis, did not significantly improve prediction of behavior change. Accordingly, these results support the idea that messages that promote a sense of personal relevance, risk perception, or related psychological processes appear related to the engagement of C₃ and C₄ and are especially apt to motivate behavior change. Indeed, several fMRI studies suggest that message-evoked brain responses in mediofrontal regions are associated with behavior change, e.g., in the context of smoking or sunscreen use (Chua et al., 2011; Falk et al., 2010, 2011, 2015). Although the current results are consistent with this work, we emphasize the need for further research and replication using larger sample sizes. For example, the different measures of alcohol consumption employed in the current study revealed variance in the behavioral outcomes - possibly due to differing temporal resolution of the measures or intra-subject variability. In this respect, more fine-grained behavioral measures, such as ecological momentary assessment could improve both the resolution and the accuracy of assessing changes in alcohol consumption over

time (e.g., [Smith et al., 2017](#)).

In general, however, the current approach reveals potential to elucidate how strong messages prompt changes - first, in receiver's brains and then in subsequent health behavior. This result also speaks directly to recent work by [Huskey et al. \(2017\)](#) and [Weber et al. \(2014\)](#), who used a brain-as-predictor approach to predict perceptions of message effectiveness in aggregate audiences. Our study complements this work, first by examining the effects of high and low PME messages on audience brain responses, second by suggesting EEG-ISC as a new, versatile method, and third by the result of the exploratory brain-as-predictor analysis. In sum, the concerted use of self-report, behavioral measures and neural data promises a window onto the pathways through which messages become affectively charged, motivate preventive health action, and ultimately to predict changes in behavior and thus, positive societal outcomes (e.g., [Falk et al., 2010](#); [Falk et al., 2015](#); [Falk et al., 2016](#); [Weber et al., 2018](#)). Although this theorizing appears plausible, we note that more work is needed to reveal the functional significance of this putative marker of collective engagement.

4.6. Correspondence between EEG- and fMRI-ISC

Beside identifying neural regions that are related to the success of health messages, our analysis linking EEG-ISC to BOLD signal measured in a second, independent target audience enables to replicate and validate the measure with respect to previous findings. For example, primary and secondary visual and auditory cortices were related to fluctuations in ISC of EEG data. Especially with regard to C₁, these findings agree with previous work using purely auditory stimulation ([Cohen and Parra, 2016](#); [Iotzov et al., 2017](#)) and work relating fluctuations within the same component to luminance changes in a video ([Poulsen et al., 2017](#)) - replicating that both primary visual and auditory processing seem to contribute to this component. Importantly, the findings of the EEG-informed analysis revealed a broad overlap with fMRI-ISC of previous work in both sensory-perceptual and cortical midline brain regions (see [Fig. 4](#) and [Imhof et al., 2017](#)). However, because the data sets were collected from different samples and not using simultaneous measurements, we cannot definitely infer that EEG-ISC is originating from the indicated brain regions. Future research collecting EEG and fMRI data from the same participants would provide more conclusive evidence regarding this issue. At the same time, however, the present analysis based on independent samples precludes that relations between the two measured modalities are the result of common physiological confounds or artifacts unrelated to the stimuli, e.g., respiration or heartbeat. The ability to integrate responses to the same set of messages across multiple modalities offers a promising strategy not only for methodological integration (e.g., [Haufe et al., 2018](#); [Liu et al., 2017](#)), but also replicates and validates the findings of enhanced ISC for strong health messages across two neuroscientific methods. This suggests that, irrespective of the neuroscientific measure, neural signals are reliably entrained across viewers by health messages. As different modalities capture independent levels of information, this approach can boost our ability to identify messages that are likely to be effective at scale.

4.7. Conclusions

In summary, the present findings demonstrate the potential of EEG-based audience response measurement to differentiate between strong and weak health messages. Beyond informing basic science questions regarding the neurocognitive processes that mediate effective messaging strategies, neural metrics of audience engagement could also be used to select promising messages from a pool of candidates, or to predict impact in audiences beyond the neuroscience laboratory. While not specifically designed for predicting audience impact, the observation that the degree of ISC captured by "higher-order components" was related to behavior change seems noteworthy. Given that health messages are a key strategy of public health prevention, developing neural measures as a proximal

marker for health message success seems promising for a translation to applied settings.

Declaration of Competing interest

The authors declare no competing interests.

Acknowledgements

We thank the Parra Lab for sharing code and expertise. We thank Tzvetan Popov, Ursula Kirmse, Tobias Flaisch, David Schubring and Karl-Philipp Flösch for valuable discussions. We also thank Martin Findler and Helena Peter for help with data collection.

Appendix A. Supplementary data

Supplementary data to this article can be found online at <https://doi.org/10.1016/j.neuroimage.2020.116527>.

Funding statement

This research was supported in part by the Deutsche Forschungsgemeinschaft (DFG, German Research Foundation) - FOR 2374 - <http://gepris.dfg.de/gepris/projekt/273711585> granted to BR and HS and the Deutsche Forschungsgemeinschaft (DFG, German Research Foundation) under Germany's Excellence Strategy - EXC2117 - 422037984.

Author contributions

MI, RS, BR & HS designed the study, MI supervised data acquisition, MI & RS carried out the statistical analysis. The manuscript was written by MI, RS & HS and all authors provided critical revisions. All authors agreed to be accountable for all aspects of the work and approved the final manuscript.

Ethics statement

All participants received either course credit or monetary reimbursement. Written informed consent was obtained according to the Declaration of Helsinki and all procedures were approved by the ethics committee of the University of Konstanz.

Data availability statement

Data to reproduce the main findings visualized in Figure 2 as well as the statistical maps visualized in Figure 3 and Figure 4 are available for download at <https://osf.io/9mc8b>. The full data that supports the findings of this study is available from the corresponding author upon reasonable request. Due to copyright restrictions and data privacy, the stimulus material as well as the raw data cannot be made publicly available. Detailed stimulus descriptions are available in previous work (<https://doi.org/10.1093/scan/nsx044>).

Code availability statement

The code that was used for the analyses is in part based on the Matlab code of the Parra Lab, which has been retrieved from <http://www.parralab.org/isc/>. The full code to reproduce figures and results is available from the corresponding author upon reasonable request.

References

- Apps, M.A.J., Rushworth, M.F.S., Chang, S.W.C., 2016. The anterior cingulate gyrus and social cognition: tracking the motivation of others. *Neuron* 90 (4), 692-707. <https://doi.org/10.1016/j.neuron.2016.04.018>.

- Babor, T.F., Higgins-Biddle, J.C., Saunders, J.B., Monteiro, M.G., 2001. AUDIT: the Alcohol Use Disorders Identification Test. Guidelines for Use in Primary Care. World Health Organization, Geneva, Switzerland. http://apps.who.int/iris/bitstream/10665/67205/1/WHO_MSD_MSB_01.6a.pdf. (Accessed 24 August 2016).
- Barnett, S.B., Cerf, M., 2017. A ticket for your thoughts: method for predicting content recall and sales using neural similarity of moviegoers. *J. Consum. Res.* 160–181. <https://doi.org/10.1093/jcr/ucw083>.
- Burns, S.M., Barnes, L.N., McCulloh, I.A., Dagher, M.M., Falk, E.B., Storey, J.D., Lieberman, M.D., 2019. Making social neuroscience less WEIRD: using fNIRS to measure neural signatures of persuasive influence in a Middle East participant sample. *J. Personal. Soc. Psychol.* <https://doi.org/10.1037/pspa0000144>.
- Cappella, J.N., 2018. Perceived message effectiveness meets the requirements of a reliable, valid, and efficient measure of persuasiveness. *J. Commun.* 68 (5), 994–997. <https://doi.org/10.1093/joc/jqy044>.
- Chua, H.F., Ho, S.S., Jasinska, A.J., Polk, T.A., Welsh, R.C., Liberzon, I., Strecher, V.J., 2011. Self-related neural response to tailored smoking-cessation messages predicts quitting. *Nat. Neurosci.* 14 (4), 426–427. <https://doi.org/10.1038/nn.2761>.
- Chua, H.F., Liberzon, I., Welsh, R.C., Strecher, V.J., 2009. Neural correlates of message tailoring and self-relatedness in smoking cessation programming. *Biol. Psychiatry* 65 (2), 165–168. <https://doi.org/10.1016/j.biopsych.2008.08.030>.
- Cohen, S.S., Henin, S., Parra, L.C., 2017. Engaging narratives evoke similar neural activity and lead to similar time perception. *Sci. Rep.* 7 (1), 4578. <https://doi.org/10.1038/s41598-017-04402-4>.
- Cohen, S.S., Madsen, J., Touchan, G., Robles, D., Lima, S.F.A., Henin, S., Parra, L.C., 2018. Neural engagement with online educational videos predicts learning performance for individual students. *Neurobiol. Learn. Mem.* 155, 60–64. <https://doi.org/10.1016/j.nlm.2018.06.011>.
- Cohen, S.S., Parra, L.C., 2016. Memorable audiovisual narratives synchronize sensory and supramodal neural responses. *eNeuro* 3 (6). <https://doi.org/10.1523/ENEURO.0203-16.2016>.
- Cooper, N., Tompson, S., O'Donnell, M.B., Emily, B.F., 2015. Brain activity in self- and value-related regions in response to online antismoking messages predicts behavior change. *J. Media Psychol.* 27 (3), 93–109. <https://doi.org/10.1027/1864-1105/a000146>.
- D'Argembeau, A., Stawarczyk, D., Majerus, S., Collette, F., van der Linden, M., Feyers, D., Maquet, P., Salmon, E., 2010. The neural basis of personal goal processing when envisioning future events. *J. Cogn. Neurosci.* 22 (8), 1701–1713. <https://doi.org/10.1162/jocn.2009.21314>.
- Davis, K.C., Duke, J.C., 2018. Evidence of the real-world effectiveness of public health media campaigns reinforces the value of perceived message effectiveness in campaign planning. *J. Commun.* 68 (5), 998–1000. <https://doi.org/10.1093/joc/jqy045>.
- Dikker, S., Wan, L., Davidesco, I., Kaggen, L., Oostrik, M., McClintock, J., Rowland, J., Michalareas, G., van Bavel, J.J., Ding, M., Poeppel, D., 2017. Brain-to-Brain synchrony tracks real-world dynamic group interactions in the classroom. *Curr. Biol.* 27 (9), 1375–1380. <https://doi.org/10.1016/j.cub.2017.04.002>.
- Dillard, J.P., Peck, E., 2000. Affect and persuasion: emotional responses to public service announcements. *Commun. Res.* 27 (4), 461–495. <https://doi.org/10.1177/009365000027004003>.
- Dillard, J.P., Weber, K.M., Vail, R.G., 2007. The relationship between the perceived and actual effectiveness of persuasive messages: a meta-analysis with implications for formative campaign research. *J. Commun.* 57 (4), 613–631. <https://doi.org/10.1111/j.1460-2466.2007.00360.x>.
- Dmochowski, J.P., Bezdek, M.A., Abelson, B.P., Johnson, J.S., Schumacher, E.H., Parra, L.C., 2014. Audience preferences are predicted by temporal reliability of neural processing. *Nat. Commun.* 5 (4567). <https://doi.org/10.1038/ncomms5567>.
- Dmochowski, J.P., Ki, J.J., DeGuzman, P., Sajda, P., Parra, L.C., 2018. Extracting multidimensional stimulus-response correlations using hybrid encoding-decoding of neural activity. *NeuroImage* 180, 134–146. <https://doi.org/10.1016/j.neuroimage.2017.05.037>.
- Dmochowski, J.P., Sajda, P., Dias, J., Parra, L.C., 2012. Correlated components of ongoing EEG point to emotionally laden attention - a possible marker of engagement? *Front. Hum. Neurosci.* 6, 112. <https://doi.org/10.3389/fnhum.2012.00112>.
- Etkin, A., Egner, T., Kalisch, R., 2011. Emotional processing in anterior cingulate and medial prefrontal cortex. *Trends Cogn. Sci.* 15 (2), 85–93. <https://doi.org/10.1016/j.tics.2010.11.004>.
- Falk, E.B., 2010. Communication neuroscience as a tool for health psychologists. *Health Psychol.* 29 (4), 355–357. <https://doi.org/10.1037/a0020427>.
- Falk, E.B., Berkman, E.T., Lieberman, M.D., 2012. From neural responses to population behavior: neural focus group predicts population-level media effects. *Psychol. Sci.* 23 (5), 439–445. <https://doi.org/10.1177/0956797611434964>.
- Falk, E.B., Berkman, E.T., Mann, T., Harrison, B., Lieberman, M.D., 2010. Predicting persuasion-induced behavior change from the brain. *J. Neurosci.* 30 (25), 8421–8424. <https://doi.org/10.1523/JNEUROSCI.0063-10.2010>.
- Falk, E.B., Berkman, E.T., Whalen, D., Lieberman, M.D., 2011. Neural activity during health messaging predicts reductions in smoking above and beyond self-report. *Health Psychol.* 30 (2), 177–185. <https://doi.org/10.1037/a0022259>.
- Falk, E.B., Cascio, C.N., Coronel, J.C., 2015. Neural prediction of communication-relevant outcomes. *Commun. Methods Meas.* 9 (1–2), 30–54. <https://doi.org/10.1080/19312458.2014.999750>.
- Falk, E.B., O'Donnell, M.B., Tompson, S., Gonzalez, R., Dal Cin, S., Strecher, V., Cummings, K.M., An, L., 2016. Functional brain imaging predicts public health campaign success. *Soc. Cogn. Affect. Neurosci.* 11 (2), 204–214. <https://doi.org/10.1093/scan/nsv108>.
- Ferrer, R., Klein, W.M., 2015. Risk perceptions and health behavior. *Curr. Opin. Psychol.* 5, 85–89. <https://doi.org/10.1016/j.copsy.2015.03.012>.
- Greenwald, A.G., Leavitt, C., 1984. Audience involvement in advertising: four levels. *J. Consum. Res.* 11 (1), 581. <https://doi.org/10.1086/208994>.
- Hasson, U., Ghazanfar, A.A., Galantucci, B., Garrod, S., Keysers, C., 2012. Brain-to-brain coupling: a mechanism for creating and sharing a social world. *Trends Cogn. Sci.* 16 (2), 114–121. <https://doi.org/10.1016/j.tics.2011.12.007>.
- Hasson, U., Landesman, O., Knappmeyer, B., Vallines, I., Rubin, N., Heeger, D.J., 2008. Neurocinematics: the neuroscience of film. *Projections* 2 (1), 1–26. <https://doi.org/10.3167/proj.2008.020102>.
- Hasson, U., Malach, R., Heeger, D.J., 2010. Reliability of cortical activity during natural stimulation. *Trends Cogn. Sci.* 14 (1), 40–48. <https://doi.org/10.1016/j.tics.2009.10.011>.
- Hasson, U., Nir, Y., Levy, I., Fuhrmann, G., Malach, R., 2004. Intersubject synchronization of cortical activity during natural vision. *Science* 303 (5664), 1634–1640. <https://doi.org/10.1126/science.1089506>.
- Haufe, S., DeGuzman, P., Henin, S., Arcaro, M., Honey, C.J., Hasson, U., Parra, L.C., 2018. Elucidating relations between fMRI, ECoG, and EEG through a common natural stimulus. *Neuroimage* 179, 79–91. <https://doi.org/10.1016/j.neuroimage.2018.06.016>.
- Haufe, S., Meinecke, F., Görgen, K., Dähne, S., Haynes, J.-D., Blankertz, B., Bießmann, F., Haufe, S., 2014. On the interpretation of weight vectors of linear models in multivariate neuroimaging. *Neuroimage* 87, 96–110. <https://doi.org/10.1016/j.neuroimage.2013.10.067>.
- Henrich, J., Heine, S.J., Norenzayan, A., 2010. The weirdest people in the world? *Behav. Brain Sci.* 33 (2–3), 61–83. <https://doi.org/10.1017/S0140525X0999152X>.
- Holmes, C.J., Hoge, R., Collins, L., Woods, R., Toga, A.W., Evans, A.C., 1998. Enhancement of MR images using registration for signal averaging. *J. Comput. Assist. Tomogr.* 22 (2), 324–333. <https://doi.org/10.1097/00004728-199803000-00032>.
- Honey, C.J., Thompson, C.R., Lerner, Y., Hasson, U., 2012. Not lost in translation: neural responses shared across languages. *J. Neurosci.* 32 (44), 15277–15283. <https://doi.org/10.1523/JNEUROSCI.1800-12.2012>.
- Huskey, R., Mangus, J.M., Turner, B.O., Weber, R., 2017. The persuasion network is modulated by drug-use risk and predicts anti-drug message effectiveness. *Soc. Cogn. Affect. Neurosci.* 12 (12), 1902–1915. <https://doi.org/10.1093/scan/nsx126>.
- Imhof, M.A., Schmäzle, R., Renner, B., Schupp, H.T., 2017. How real-life health messages engage our brains: shared processing of effective anti-alcohol videos. *Soc. Cogn. Affect. Neurosci.* 12 (7), 1188–1196. <https://doi.org/10.1093/scan/nsx044>.
- Iotzov, I., Fidalì, B.C., Petroni, A., Conte, M.M., Schiff, N.D., Parra, L.C., 2017. Divergent neural responses to narrative speech in disorders of consciousness. *Ann. Clin. Transl. Neurol.* 4 (11), 784–792. <https://doi.org/10.1002/acn3.470>.
- Karam, E., Kyprì, K., Salamoun, M., 2007. Alcohol use among college students: an international perspective. *Curr. Opin. Psychiatr.* 20 (3), 213–221. <https://doi.org/10.1097/YCO.0b013e3280fa836c>.
- Ki, J.J., Kelly, S.P., Parra, L.C., 2016. Attention strongly modulates reliability of neural responses to naturalistic narrative stimuli. *J. Neurosci.* 36 (10), 3092–3101. <https://doi.org/10.1523/JNEUROSCI.2942-15.2016>.
- Lahnakoski, J.M., Glerean, E., Jääskeläinen, I.P., Hyönä, J., Hari, R., Sams, M., Nummenmaa, L., 2014. Synchronous brain activity across individuals underlies shared psychological perspectives. *NeuroImage* 100, 316–324. <https://doi.org/10.1016/j.neuroimage.2014.06.022>.
- Lakens, D., 2013. Calculating and reporting effect sizes to facilitate cumulative science: a practical primer for t-tests and ANOVAs. *Front. Psychol.* 4, 863. <https://doi.org/10.3389/fpsyg.2013.00863>.
- Leech, R., Sharp, D.J., 2014. The role of the posterior cingulate cortex in cognition and disease. *Brain: J. Neurol.* 137 (Pt 1), 12–32. <https://doi.org/10.1093/brain/awt162>.
- Liu, Y., Piazza, E.A., Simony, E., Shewokis, P.A., Onaral, B., Hasson, U., Ayaz, H., 2017. Measuring speaker-listener neural coupling with functional near infrared spectroscopy. *Sci. Rep.* 7, 43293. <https://doi.org/10.1038/srep43293>.
- Lochbuehler, K., Tang, K.Z., Souprontchouk, V., Campetti, D., Cappella, J.N., Kozlowski, L.T., Strasser, A.A., 2016. Using eye-tracking to examine how embedding risk corrective statements improves cigarette risk beliefs: implications for tobacco regulatory policy. *Drug Alcohol Depend.* 164, 97–105. <https://doi.org/10.1016/j.drugaldep.2016.04.031>.
- Madsen, J., Margulis, E.H., Simchy-Gross, R., Parra, L.C., 2019. Music synchronizes brainwaves across listeners with strong effects of repetition, familiarity and training. *Sci. Rep.* 9, 3576. <https://doi.org/10.1038/s41598-019-40254-w>.
- McGuire, W.J., 2013. McGuire's classic input-output framework for constructing persuasive messages. In: Rice, R.E., Atkin, C.K. (Eds.), *Public Communication Campaigns*, 4th ed. SAGE, Thousand Oaks, Calif, pp. 133–145.
- Menon, V., Uddin, L.Q., 2010. Saliency, switching, attention and control: a network model of insula function. *Brain Struct. Funct.* 214 (5–6), 655–667. <https://doi.org/10.1007/s00429-010-0262-0>.
- Mesulam, M.-M., 1998. From sensation to cognition. *Brain: J. Neurol.* 121 (6), 1013–1052. <https://doi.org/10.1093/brain/121.6.1013>.
- Murray, R.J., Schaer, M., Debbané, M., 2012. Degrees of separation: a quantitative neuroimaging meta-analysis investigating self-specificity and shared neural activation between self- and other-reflection. *Neurosci. Biobehav. Rev.* 36 (3), 1043–1059. <https://doi.org/10.1016/j.neubiorev.2011.12.013>.
- O'Keefe, D.J., 2018. Message pretesting using assessments of expected or perceived persuasiveness: evidence about diagnosticity of relative actual persuasiveness. *J. Commun.* 68 (1), 120–142. <https://doi.org/10.1093/joc/jqx009>.
- O'Keefe, D.J., 2019. Message pretesting using perceived persuasiveness measures: reconsidering the correlational evidence. *Commun. Methods Meas.* 28, 1–13. <https://doi.org/10.1080/19312458.2019.1620711>.
- Ostenveld, R., Fries, P., Maris, E., Schoffelen, J.-M., 2011. FieldTrip: open source software for advanced analysis of MEG, EEG, and invasive electrophysiological data. *Comput. Intell. Neurosci.* 2011, 156869. <https://doi.org/10.1155/2011/156869>.

- Palmgreen, P., Stephenson, M.T., Everett, M.W., Baseheart, J.R., Francies, R., 2002. Perceived message sensation value (PMSV) and the dimensions and validation of a PMSV scale. *Health Commun.* 14 (4), 403–428. https://doi.org/10.1207/S15327027HC1404_1.
- Parra, L.C., Haufe, S., Dmochowski, J.P., 2018. Correlated components analysis - extracting reliable dimensions in multivariate data. arXiv. <https://arxiv.org/abs/1801.08881v4>.
- Parra, L.C., Spence, C.D., Gerson, A.D., Sajda, P., 2005. Recipes for the linear analysis of EEG. *Neuroimage* 28 (2), 326–341. <https://doi.org/10.1016/j.neuroimage.2005.05.032>.
- Petty, R., Cacioppo, J., 1986. The elaboration likelihood model of persuasion. *Adv. Exp. Soc. Psychol.* 19, 123–205. [https://doi.org/10.1016/S0065-2601\(08\)60214-2](https://doi.org/10.1016/S0065-2601(08)60214-2).
- Pei, R., Schmälzle, R., Kranzler, E.C., O'Donnell, M.B., Falk, E.B., 2019. Adolescents' neural response to tobacco prevention messages and sharing engagement. *Am. J. Prev. Med.* 56 (2S1), S40–S48. <https://doi.org/10.1016/j.amepre.2018.07.044>.
- Petty, R.E., Brinol, P., Priester, J.R., 2009. Mass media attitude change: implications of the elaboration likelihood model of persuasion. In: Bryant, J., Oliver, M.D. (Eds.), *Media Effects. Advances in Theory and Research*, 3rd ed. Routledge, New York, pp. 125–164.
- Poldrack, R.A., 2006. Can cognitive processes be inferred from neuroimaging data? *Trends Cogn. Sci.* 10 (2), 59–63. <https://doi.org/10.1016/j.tics.2005.12.004>.
- Poulsen, A.T., Kamronn, S., Dmochowski, J., Parra, L.C., Hansen, L.K., 2017. EEG in the classroom: synchronised neural recordings during video presentation. *Sci. Rep.* 7, 43916. <https://doi.org/10.1038/srep43916>.
- Qin, P., Northoff, G., 2011. How is our self related to midline regions and the default-mode network? *Neuroimage* 57 (3), 1221–1233. <https://doi.org/10.1016/j.neuroimage.2011.05.028>.
- Raichle, M.E., 2015. The brain's default mode network. *Annu. Rev. Neurosci.* 38, 433–447. <https://doi.org/10.1146/annurev-neuro-071013-014030>.
- Renner, B., 2004. Biased reasoning: adaptive responses to health risk feedback. *Personal. Soc. Psychol. Bull.* 30 (3), 384–396. <https://doi.org/10.1177/0146167203261296>.
- Renner, B., Gamp, M., Schmälzle, R., Schupp, H.T., 2015. Health risk perception. In: Wright, J.D. (Ed.), *International Encyclopedia of the Social and Behavioral Sciences*. Elsevier, Amsterdam, pp. 702–709.
- Renner, B., Reuter, T., 2012. Predicting vaccination using numerical and affective risk perceptions: the case of A/H1N1 influenza. *Vaccine* 30 (49), 7019–7026. <https://doi.org/10.1016/j.vaccine.2012.09.064>.
- Rice, R.E., Atkin, C.K. (Eds.), 2013. *Public Communication Campaigns*, 4th ed. SAGE, Thousand Oaks, Calif.
- Rumpf, H.-J., Hapke, U., Meyer, C., John, U., 2002. Screening for alcohol use disorders and at-risk drinking in the general population: psychometric performance of three questionnaires. *Alcohol Alcohol* 37 (3), 261–268. <https://doi.org/10.1093/alcac/37.3.261>.
- Schmälzle, R., Häcker, F.E., Renner, B., Honey, C.J., Schupp, H.T., 2013. Neural correlates of risk perception during real-life risk communication. *J. Neurosci.* 33 (25), 10340–10347. <https://doi.org/10.1523/JNEUROSCI.5323-12.2013>.
- Schmälzle, R., Häcker, F.E.K., Honey, C.J., Hasson, U., 2015. Engaged listeners: shared neural processing of powerful political speeches. *Soc. Cogn. Affect. Neurosci.* 10 (8), 1137–1143. <https://doi.org/10.1093/scan/nsu168>.
- Schmitz, T.W., Johnson, S.C., 2007. Relevance to self: a brief review and framework of neural systems underlying appraisal. *Neurosci. Biobehav. Rev.* 31 (4), 585–596. <https://doi.org/10.1016/j.neubiorev.2006.12.003>.
- Seeley, W.W., Menon, V., Schatzberg, A.F., Keller, J., Glover, G.H., Kenna, H., Reiss, A.L., Greicius, M.D., 2007. Dissociable intrinsic connectivity networks for salience processing and executive control. *J. Neurosci.* 27 (9), 2349–2356. <https://doi.org/10.1523/JNEUROSCI.5587-06.2007>.
- Shackman, A.J., Salomons, T.V., Slagter, H.A., Fox, A.S., Winter, J.J., Davidson, R.J., 2011. The integration of negative affect, pain and cognitive control in the cingulate cortex. *Nat. Rev. Neurosci.* 12 (3), 154–167. <https://doi.org/10.1038/nrn2994>.
- Silbert, L.J., Honey, C.J., Simony, E., Poeppel, D., Hasson, U., 2014. Coupled neural systems underlie the production and comprehension of naturalistic narrative speech. *Proc. Natl. Acad. Sci. U.S.A.* 111 (43), E4687–E4696. <https://doi.org/10.1073/pnas.1323812111>.
- Slovic, P., Peters, E., 2006. Risk perception and affect. *Curr. Dir. Psychol. Sci.* 15 (6), 322–325. <https://doi.org/10.1111/j.1467-8721.2006.00461.x>.
- Slutske, W.S., 2005. Alcohol use disorders among US college students and their non-college-attending peers. *Arch. Gen. Psychiatry.* 62 (3), 321–327. <https://doi.org/10.1001/archpsyc.62.3.321>.
- Smith, A., de Salas, K., Lewis, I., Schütz, B., 2017. Developing smartphone apps for behavioural studies: the AlcoRisk app case study. *J. Biomed. Inform.* 72, 108–119. <https://doi.org/10.1016/j.jbi.2017.07.007>.
- Stephens, G.J., Silbert, L.J., Hasson, U., 2010. Speaker-listener neural coupling underlies successful communication. *Proc. Natl. Acad. Sci. U.S.A.* 107 (32), 14425–14430. <https://doi.org/10.1073/pnas.100862107>.
- Talairach, J., Tournoux, P., 1988. *Co-planar stereotaxic atlas of the human brain: 3-dimensional proportional system; an approach to cerebral imaging*. Thieme Medical Publishers, New York.
- Wakefield, M.A., Loken, B., Hornik, R.C., 2010. Use of mass media campaigns to change health behaviour. *The Lancet* 376 (9748), 1261–1271. [https://doi.org/10.1016/S0140-6736\(10\)60809-4](https://doi.org/10.1016/S0140-6736(10)60809-4).
- Wang, A.-L., Ruparel, K., Loughead, J.W., Strasser, A.A., Blady, S.J., Lynch, K.G., Romer, D., Cappella, J.N., Lerman, C., Langenbrenner, D.D., 2013. Content matters: neuroimaging investigation of brain and behavioral impact of televised anti-tobacco public service announcements. *J. Neurosci.* 33 (17), 7420–7427. <https://doi.org/10.1523/JNEUROSCI.3840-12.2013>.
- Weber, R., Fisher, J.T., Hopp, F.R., Lonergan, C., 2018. Taking messages into the magnet: method–theory synergy in communication neuroscience. *Commun. Monogr.* 85 (1), 81–102. <https://doi.org/10.1080/03637751.2017.1395059>.
- Weber, R., Huskey, R., Mangus, J.M., Westcott Baker, A., Turner, B.O., 2014. Neural predictors of message effectiveness during counterarguing in antidrug campaigns. *Commun. Monogr.* 82 (1), 4–30. <https://doi.org/10.1080/03637751.2014.971414>.
- Weber, R., Westcott Baker, A., Anderson, G., 2013. A multilevel analysis of antimarijuana public service announcement effectiveness. *Commun. Monogr.* 80 (3), 302–330. <https://doi.org/10.1080/03637751.2013.788254>.
- Weinstein, N.D., 1989. Effects of personal experience on self-protective behavior. *Psychol. Bull.* 105 (1), 31–50. <https://doi.org/10.1037/0033-2909.105.1.31>.
- Wicki, M., Kuntsche, E., Gmel, G., 2010. Drinking at European universities? A review of students' alcohol use. *Addict. Behav.* 35 (11), 913–924. <https://doi.org/10.1016/j.addbeh.2010.06.015>.
- Yzer, M., LoRusso, S., Nagler, R.H., 2015. On the conceptual ambiguity surrounding perceived message effectiveness. *Health Commun.* 30 (2), 125–134. <https://doi.org/10.1080/10410236.2014.974131>.
- Zhao, X., Strasser, A., Cappella, J.N., Lerman, C., Fishbein, M., 2011. A measure of perceived argument strength: reliability and validity. *Commun. Methods Meas.* 5 (1), 48–75. <https://doi.org/10.1080/19312458.2010.547822>.